Journal of
Renewable Energy Research and Applications (RERA)

Vol. 3, No. 1, 2022, 51-59 *DOI: 10.22044/rera.2021.11122.1074*

CFD Analysis of Vertical Axis Wind Turbine with Winglets

Sharul Sham Dol*, Abdullah Khamis, Mohanad Tarek Abdallftah, Mohammed Fares and Salman Shahid

Department of Mechanical Engineering, Abu Dhabi University, Abu Dhabi, UAE.

Receive Date 19 August 2021; Revised 01 September 2021; Accepted Date 18 September 2021
**Corresponding author: ab@etc (Sh.Sh. Dol)*

Abstract

The current research work illustrates the optimization of Vertical Axis Wind Turbine (VAWT) blades with implementation of added winglets displaying improved self-starting capabilities. The application of improved design is to be utilized in a university campus located in the United Arab Emirates (UAE) in order to reduce its margin of consumed electrical energy by 15%. This work is conducted over a mean wind speed value of 5 m/s achieved in a one-year period at a specific altitude of 50 m in the UAE. Two aerodynamic simulation softwares are adopted, namely ANSYS FLUENT CFD and QBlade, with designs being modelled using AutoCAD. The analytical analysis includes some aerodynamic characteristics such as power, lift, and drag coefficients. Through 2D-computational fluid dynamics (CFD), the simulation study tests 20 different symmetrical as well as asymmetrical airfoils including the cambered S-0146 with 26.83% higher power output and lower noise amongst the test subjects. Turbine torque for the added winglet design results in 4.1% higher compared to the benchmark. The modified design aims to produce at least 2% more power, and has an improvement in self-starting of at least 20%. VAWTs tend to have a higher potential and sensitivity towards wind direction (no yawing mechanism required), illustrating them as more cost-effective. The future scope includes utilizing the wind lens technology to increase the free-stream velocity.

Keywords: *Vertical axis wind turbine, Aerodynamics, Lift, Drag, Computational fluid dynamics, Winglet, Blade, Power transmission, Self-starting, Angle-of-Attack.*

1. Introduction

Presently, substantial efforts have been made in greening the energy sector by transferring the application of fossil fuels to renewable energy with an intent to reduce the fossil fuel usage. Wind is an ideal alternate source of energy, providing a limitless amount of clean energy for numerous applications [1]. Advanced markets based upon the wind energy technology have emerged with the means to efficiently transform available wind energy to a practical form of energy such as electricity. The primary core of this technology consists of the wind turbine, a type of turbomachinery that transfers mechanical energy through blades converting one form of energy to another [2]. The potential of wind is distributed unevenly throughout the world with the northern and western parts experiencing higher winds compared to the southern parts, illustrating that the conventional wind turbines cannot provide similar performance throughout.

Vertical Axis Wind Turbines (VAWTs) can be altered to improve the performance as well as the self-starting capabilities [3]. Additional information can be discovered in [4].

Recently, the UAE has developed the International Renewable Energy Agency (IRENA) as well as the Emirates Nuclear Energy Corporation (ENEC) with the development of a revolutionary city named Masdar city; its precise geographical location is illustrated in figure 1. It operates effectively with a clean and sustainable energy promoting wide-scale projects for renewable sources over 30 distinct countries [5]. Masdar has delivered unprecedented wind energy plants across the Persian Gulf region retrieving 50 MW of output power solely through wind turbines. The Dhofar wind power place located in the Dhofar city (Oman) powers over 15,000 homes and represents 7% of the Dhofar Governate's electricity [6]. Presently, the horizontal wind turbines are predominantly utilized in plants; however, the proposed model illustrating a higher potential would allow it to be utilized at a mass-scale [7].

Figure 1. Masdar city geographical location [8].

Regarding the multiple methods to sustain renewable energy, wind turbines are recognized as the most effective means of renewable energy. Wind is acquired free of cost, pure, and never ending; in addition to that, the instalment of wind power plant is relatively cheap compared to the other power plants. More information can be obtained in [9]. Wind turbines are categorized into two types, Horizontal Axis Wind Turbine (HAWT) and Vertical Axis Wind Turbines (VAWT). The selection of one depends upon the market demand and application. At the present time, HAWTs exceed VAWTs in terms of marketing, as the horizontal designs have been manufactured prior to the vertical ones, thus providing additional experience and field assessment [10].

VAWTs are recognized to consist of deprived self-starting capabilities, as at low velocities, the turbine entails large starting torque to commence steady rotation lowering overall turbine efficiency along with reliability [11]. This research work enhances the self-starting performance of a VAWT without impacting its power generation performance. The developed design will expectantly cover 15% of the entire energy consumption for a university campus in the UAE [12].

The structural scheme in figure 2 illustrates a straight bladed VAWT that appears as an alphabetic letter “H”, hence its name H-rotor VAWT; furthermore, the structural components are simpler than Troposkien VAWT, making them relatively cheaper. The design consists of 2 to 6 blades depending upon the application [13].

These VAWTs have been recognized to have complications in self-starting along with a noise during operation. Overcoming these challenges with an active passive flow control is crucial, and can be applied for management of blade tip vortex as well as dynamic stall. The active flow control applies self-flow injection channels, whereas the passive flow includes winglet and grooves at the blade tip. The factors such as aero-elasticity that refer to the interaction between the inelastic and aerodynamic forces are considered crucial for the wind turbine stability as well as its life-time reliability [15].

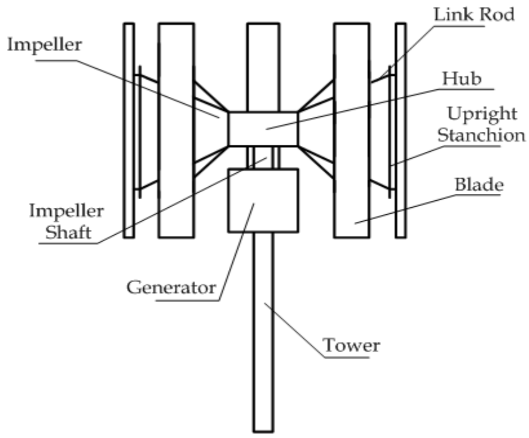

Figure 2. H-rotor VAWT [14].

Ensuring effective wind turbines, this research work studies wind speed that fuels the system for generation of electricity. An average deduction of wind speed in the UAE opts to 5 m/s, whereas, in the winter season, the speed enhances as winds are stronger, and reach 10 m/s. figure 3 demonstrates the mean wind speed recorded in 2015 at a height of 50 m above the sea level in the UAE [16]. The data retrieved is crucial in designing a wind turbine that is appropriate for the considered application in the project; furthermore, turbine installation is eligible on the ground or over buildings and houses. Thus employment of small-scale turbines must be examined; in addition to this, the aerodynamic performance must be enhanced to surge effectiveness and extract higher amounts of wind power for utilization of electrical energy.

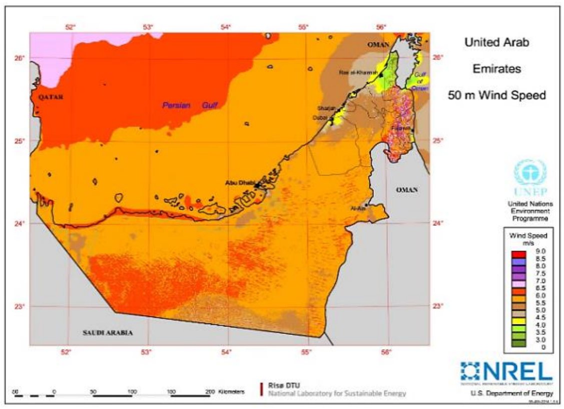

Figure 3. Mean wind speed in the UAE at a 50 m height [16].

This research work aims at optimization of VAWT blades to illustrate improved self-starting capabilities through employment of winglet at blade tips. Its application is aimed to be utilized at a university campus located in the UAE in an effort to replace a small margin of the consumed electrical energy (15%) powered by the typical non-renewable resources. The initial theoretical test involves aerodynamic characteristics such as lift and drag coefficient as well as power. The structural layout of the final design including blades, struts, rotating shaft, and tower design is also investigated; in addition to that, this paper highlights the materials to be applied. The final design aims at improving self-starting capabilities of a VAWT by a minimum of 20% with all designs simulated in ANSYS Fluent at specific velocities.

Zhang et al. (2019) [17], have highlighted that tip vortices experience due to traditional VAWT blade diminish power efficiency, and thus the implementation of winglets. They reduced the computational cost through limiting the simulation to a one-blade oscillating problem. According to their orthogonal experiment design, twist angle of winglet is a crucial factor that impacts the winglet performance. They illustrated that implementation of winglet reduces tip vortices and improves wind turbine performance by 31%.

Javadi et al. (2017) [18] have focused on self-starting characteristics for Darrieus-type VAWTs. They proposed a numerical simulation method considering the turbines moment of inertia. Their simulation begins from an initial stationary state, and operates until a steady-periodic motion is maintained. Their results illustrated an increase in rotor inertia indicating that turbine took longer to reach the final velocity. They also indicated that at a rotor TSR of greater than 1.0, blade vortices diminish and generate higher lift force, resulting in an increase in acceleration.

Lain et al. (2018) [19], have studied three-dimensional numerical simulation of flow around VAWTs. They studied turbine performance through time-accurate Reynolds Averaged Navier Stokes commercial solver utilizing NACA0025 Airfoil modified with added winglets at blade tips in order to eliminate the trailing vortices strength. They utilized several turbulence models in their computational numerical model including SST and Reynolds Stress model. Addition of winglets results in an increase in the thrust as well as an increase in the torque.

2. Design Parameters

Computational Fluid Dynamics (CFD) is an influential approach towards the evaluation and optimization of the wind turbine performance; however, to commit on the reliability and verification for the data obtained, it is recommended to perform a wind tunnel testing, and to compare the numerical results with the experimental data. According to a study “CFD simulations of power coefficients for an innovative Darrieus style vertical axis wind turbine with auxiliary straight blades” [20], simulations were performed through the CFD examination of the Darrieus-type vertical axis micro-wind turbine consisting of a straight-blade configuration designed, specifically for small-scale conversion of energy in terms of low wind speeds. Dominy et al. (2006) [21] have stated that Darrieus turbine is characteristically non-self-starting; however, this can be tackled through a careful selection of airfoil.

2.1. Blade Profile

The initial VAWT research work primarily considered symmetrical NACA00xx as well as NACA0012, NACA0015 and NACA0018. These profiles were quite desired and well-recognized with the data availability of numerous conditions; however, these profiles were mainly developed for the aviation applications. This sparked a requirement for the development of a well-suited profile for VAWT. This led to the evolution of laminar flow airfoils, cambered airfoils as well as increased thickness airfoils. Additional information can be found in [22].

Through 2D computational fluid dynamics, the simulation study tested 20 different symmetrical as well as asymmetrical airfoils including the cambered S-0146 with 26.83% higher power output and lower noise amongst the test subjects; furthermore, it was recognized that enhanced solidity as well as tip speed ratio surged noise. With respect to this, comparing DU06W200 (airfoil with 20% thickness and 0.8% camber) together with NACA0018, it was discovered that applying DU06W200 airfoil results in 5% increase peak power output [23].

Based on the decision matrix in table 1, glass fiber reinforced plastic would be the top choice for the VAWT blade material. Glass fiber-reinforced plastics (GRP) are a common composite material utilized in the wind turbine industry, due to GRP providing crucial properties including the mechanical and non-mechanical preterits at a lower cost. E-glass is the most applied glass in manufacturing reinforced fibers due to its water absorption rate properties and efficient insulation [24].

Table 1. Material selection decision matrix.

Design parameters	Weight	Structural steel	Aluminum	Carbon fiber	Glass fiber reinforced plastic
Resistance to corrosion	15%	2	4	5	5
Strength	20%	3	2	5	4
Resistance to fatigue	20%	3	2	5	4
Ease of manufacturing	10%	4	4	1	5
Manufacturing cost	15%	4	3	1	3
High-Temperature Tolerance	5%	2	2	4	2
Eco-friendly	10%	4	4	1	2
Density	5%	1	3	4	3
Total	100%	3.05	2.9	3.5	3.75

2.2 Blade Design

This research work tests NACA 0015, NACA 0018, NACA 0021, NACA 4412, and NACA 23015. Some airfoils take roots from the DU families with their maximum airfoil thickness to chord percentage attaining 40%. Initially, they are modelled through the RFOIL software that utilizes XFOIL code in order to obtain a maximum lift generation [25]. The range of angle of attacks is selected from -10° to 20° with increments of 0.5°. The analysis considers the Reynolds and Mach number set at 63291 and 0.01, respectively. Running the analysis results in retrieval of lift and drag coefficient, lift/drag ratio with respect to the angle of attack figures. First, the turbine blade length was assigned as the reference blade length as depicted in figure 4.

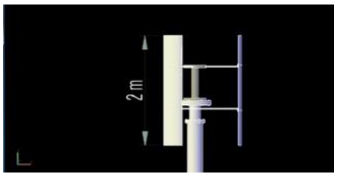

Figure 4. AutoCAD drawing of benchmark blade length.

The shaft length is set to 8.6 m, whereas the outer tower diameter is 0.09 m. The tower length is set as 7.6 m while the inner diameter is 0.105 m. figure 5 demonstrates an isometric view of the benchmark design illustrating a normal VAWT design with no additional alteration or modification to blades.

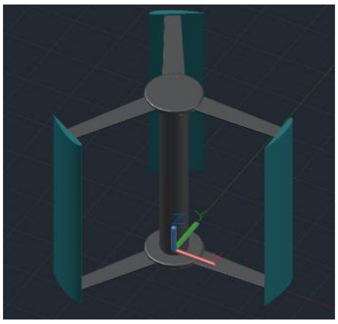

Figure 5. Isometric view of benchmark design in ANSYS.

2.3 Winglets Addition to Benchmark Design

Winglet addition reduces the drag and delivers an additional lift; furthermore, the drag reduction rates for winglets can reach as high as 5; in addition to that, applying the blended winglet configuration enables a smooth shifting of chord distribution from wingtip to winglet, resulting in the optimization of span load lift distribution and diminishing any aerodynamic disturbance or separation of flow [26]. Based on the experimental study, adding winglets increases the power coefficient by 10 to 19 percent; in addition, a higher output torque (+12.8%) could be generated at an infinite azimuth angle in a circle [27]. 54

Based on the winglet design, the root chord length is 400 mm with an inclination angle of 30°, a lead edge sweep angle of 42°, and a winglet height of 200 mm, as shown in figure 6.

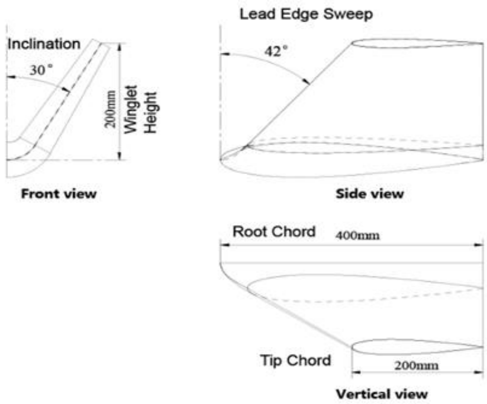

Figure 6. Winglet design dimensions.

The isometric view of the geometry utilized in ANSYS for the new design is illustrated in figure 7 as AutoCAD drawing.

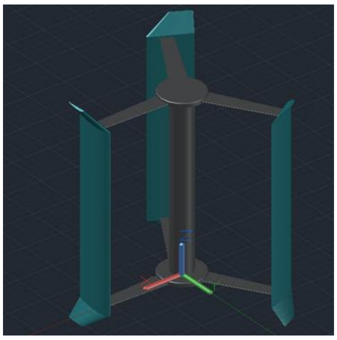

Figure 7. Isometric winglet design.

3. Boundary Conditions

A crucial phase in the research work is to determine the wind speed at which the wind turbine operates. It will contribute in predicting the performance of designed wind turbine. For the provided swept area, the available kinetic energy in the wind can be calculated using (1).

$$\mathrm{P_w} = \frac{1}{2}\rho \mathrm{A} \mathrm{V}_\infty^3 \quad (1)$$

Where density is noted as 'ρ', and wind speed 'V_∞', and 'A' defines the swept area that is the area at which the wind turbine rotor blades spin. Considering a VAWT, the swept area can be calculated through $2RH$, where "R" is the rotor radius, while "H" is blade height. The available wind energy is extracted by wind due to Betz limit as well as the efficiency of designed wind turbine. Max power can be extracted by wind turbine equaling to $0.59P_w$; however, the amount of available wind power can be improved through enhancement in the swept area by increasing the diameter or height of the wind turbine leading to an increase in the kinetic energy of wind [28].

With respect to the rotor rotation, the local azimuth angle for each blade differs leading to changes in the relative wind (W) as well as the angle of attack (α) that can be calculated through (2).

$$\alpha = \tan^{-1}\left[\frac{\sin\theta}{\lambda/(V_i/V_\infty) + \cos\theta}\right] \quad (2)$$

where θ is the azimuth angle and (V_i/V_∞) is the ratio of the induced velocity to freestream velocity. Observing the equation of angle of attack, minor tip speed ratio value led to higher angle of attacks; however, higher tip speed ratios result in lower angle of attacks; therefore, the tip speed ratio must be calculated prudently, avoiding aerodynamic stall in wind turbine caused by large disparities in α.

The meshing consists of a global element sizing of 0.15 m selected at a maximum size of 0.25 m including a higher smoothing in quality. The model utilized three meshing methods controlling the mesh sizing effectively, mainly through body sizing, face sizing, and inflation. Body sizing is applied on rotating domain in order to reduce the element size to 0.05 m, whereas face sizing is utilized on the turbine walls for the control and further reduction in element size (i.e to 0.01 m); furthermore, inflation consists of rotating domain with turbine wall boundary that refines mesh along the turbine walls. Figure 8 depicts the mesh distribution over the turbine model.

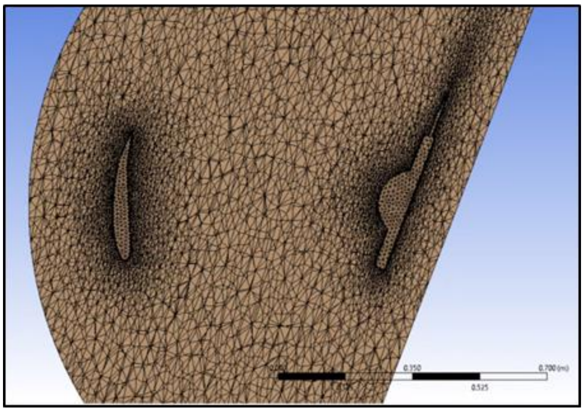

Figure 8. Turbine wall mesh distribution.

The model setup involves the solver type as pressure-based alongside transient solver. The SST *k-ω* turbulence model is designated for a viscous model in this research work as it provides a solution agreeing with the experimental data [29]. In terms of the computational models, three standard aerodynamic models are considered such as the momentum model, vortex model, and cascade model. The models are primary elements in defining the optimization required in the individual parameters [30].

Based on a literature survey, Tip-Speed Ratio (TSR) is referred to the turbine linear velocity over wind velocity, and due to TSR providing the highest power coefficient of 2.5, it is selected as this designs TSR followed by linear velocity.

4. Results and Discussion

CFD simulation can be fine-tuned as the small timestep overcoming problems of force and torque; in addition to this, information is retrieved directly from the simulation at the specified sample rate [31]. Utilizing ANSYS CFD, the velocity vectors were illustrated to analyze the fluid particle velocities at different points close to the turbine walls; furthermore, the static pressure and velocity contours around the turbine wall for both designs. Figure 9 illustrates the moment with respect to time graph for the benchmark design.

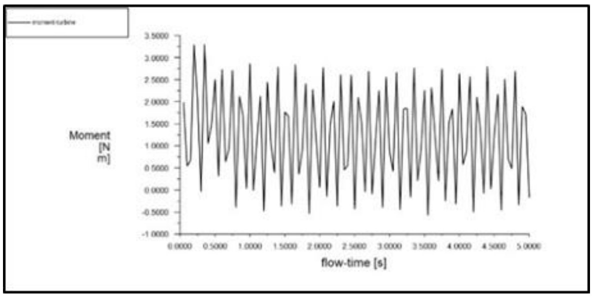

Figure 9. Moment vs. flow time – benchmark.

Utilizing figure 9, the turbine torque can be calculated as per (3).

$$\text{Turbine torque} = 0.9555 + 1.25 = 2.2055 \text{ (Nm)} \quad (3)$$

Whereas figure 10 illustrates the moment vs. flow time for the added winglet design.

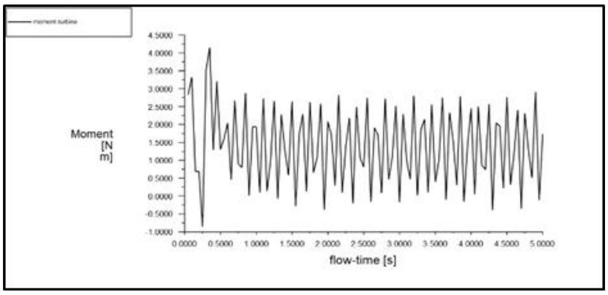

Figure 10. Moment vs. flow time – benchmark.

The turbine torque is calculated as per (4).

$$\text{Turbine torque} = 0.79625 + 1.5 = 2.29625 \text{ (Nm)} \quad (4)$$

As per (3) and (4), the turbine torque for added winglet design is higher compared to the benchmark design depicting a 4.1% increase in torque. Table 2 summarizes the CFD results including the lift and drag force for both the benchmark and design 2 for comparison.

Table 2. CFD retrieved results for benchmark and added winglet design.

Design parameters	Benchmark	Design 2 (Addition of winglet)
Torque generated (N.m)	2.2055	2.29625
Lift force (N)	9.555	4.555
Drag force (N)	99.555	116.37
Lift/Drag ratio	0.096	0.039
Power generated (W)	35.3	36.7
Self-Starting torque (N.m) (Max torque reached within 0.5 s)	3.25	4.1

As per table 2, the generated torque surpasses the benchmark after implementation of winglets, while the lift force is reduced to 4.55 N from 9.55 N, the drag force faces an increase to 116.37 N. The lift-to-drag ratio demonstrates a reduction from 0.096 to 0.039; however, a primary increase is shown in the generated power from 35.3 to 36.7 Watts. Figure 11 illustrates the velocity vectors for the benchmark and the added winglets design.

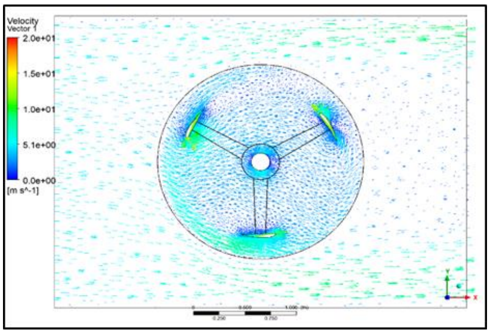

Figure 11. Velocity vector – benchmark design.

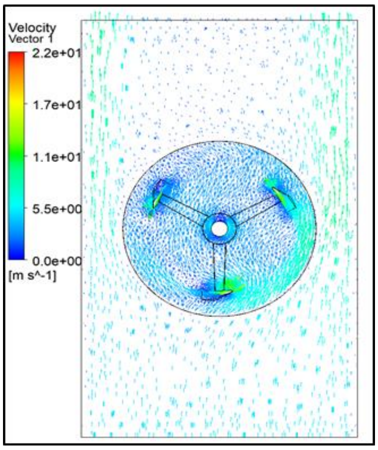

Figure 12. Velocity vector – added winglet design.

By observing the bottom airfoil for each design illustrated in figures 11 and 12, the figures illustrate a higher velocity magnitude with added winglets compared to the benchmark design. Figures 13 and 14 illustrate a closer look at the velocity vector from the bottom airfoil. The near-tip streamlines followed from upstream of reference blade tend to transfer from pressure side to suction side at the tip. This diminishes the pressure difference between the two sides of the blade not allowing the blade to generate sufficient thrust. The winglet separates the blade tip restricting streamlines from crossing over maintaining the pressure difference between both sides; this further improves the aerodynamic efficiency at the blade tip [17].

As observed in the regions highlighted by blue rectangles (airfoil experience approximately similar angle of attack with respect to the upcoming flow). It is recognized that the winglet design depicts a higher flow separation (larger wake region) explaining the high amounts of drag. It further recognizes the air flow near airfoil indicating a higher skin friction that accords to an elevation in overall drag, which is expected, as the winglet design has a higher surface area. The figures illustrate that implementation of winglet shifting the distribution of the vorticity field, further diminishing the intensity as well as influencing the tip vortex [17].

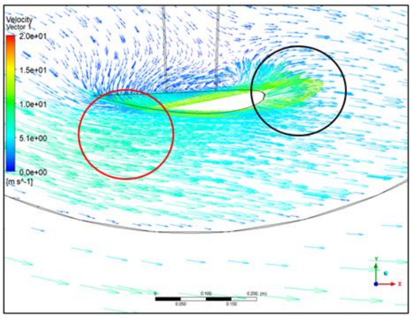

Figure 13. Velocity vector – benchmark bottom airfoil.

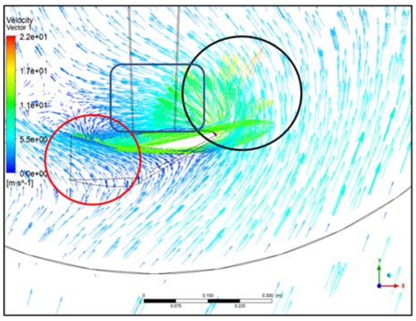

Figure 14. Velocity vector – added winglet bottom airfoil.

Based upon figure 13, the velocity vectors are aligned parallel to airfoil; leading edge of airfoil presents higher magnitude vectors (illustrated in a black circle); however, the external wind approaching towards the airfoil does not fully support the motion, and rather gets disperse (depicted in a red circle). Figure 14 depicts similar observations since high velocity magnitude vectors at the leading edge of airfoil (black circle) in the rotational direction; whereas, at the trailing edge of airfoil, the vectors consisting of a less magnitude act in the opposite direction exerting drag. Flow separation directly impacts the pressure distribution over the surface of the blade disrupting pitch balance in the flow process; moreover, due to flow separation, the flow is highly unstable as per generated vortices leading to heightened noise generation [32]. The added winglet design depicts a higher drag, and is concentrated with a close alignment in the opposite direction.

It must be noted that adding winglet at the blade tip improves the torque contribution along the blade span. There is a larger enhancement at the blade tip since the pressure difference at the blade tip signifies a higher impact on the blade surface located closer to the tip [17].

Figure 15 illustrates the location of VAWT in the Abu Dhabi University (ADU) – Al Ain Campus with the VAWT placed in an open area with a significant wind flow allowing it to operate for a longer period of time.

Figure 15. Location of VAWT in ADU-AA campus.

4.1. Power Consumption

The electricity consumption of a university campus in the UAE in the year 2020 is illustrated in table 3. The estimated number of working hours in the university per week is 63 hours including 11 hours per day in the working days, while 4 hours per day in the weekend. The total power consumption amounts to 1723.7 kW, and since the design must provide 15% of the total power consumption, with each turbine provides about 6 kW, the total amount of turbine required is 43.

Table 3. Electricity consumption in the Abu Dhabi University – Abu Dhabi campus.

Month	YEAR 2020	YEAR 2019
	Consumption (KILOWATT-HR)	Consumption (KILOWATT-HR)
January	575,178	590,208
February	537,048	560,810
March	506,922	632,423
April	365,036	635,008
May	409,235	660,373
June	428,998	651,812
July	478,512	672,596
August	514,775	633,941
September	490,836	705,486
October	498,295	706,708
November	442,085	612,757
December	400,033	536,409
TOTAL	**5,646,953**	**7,598,531**

5. Conclusion

This research work is aimed to be functional in a university campus located in the United Arab Emirates; in the UAE, hopes of renewable energy are emerging, and the movement has been initiated in the past. The objectives of this research work stated optimizing the performance of VAWT, specifically the H-type Darrieus through an aerodynamic analysis. The methodology shadowed a comprehensive research work on wind turbines as well as their applications, theoretical design, and number of modifications tested in ANSYS to select the best fit along with the specifications of the final design. A number of VAWT were positioned close to each other (higher density) in precise areas in order to generate higher amounts of power. VAWTs tend to portray a higher efficiency than HAWTs.

It was discovered that the self-starting capability in VAWTs was an exponential drawback that drove most applications to continuing relying upon HAWTs; however, VAWTs tend to have a higher potential and sensitivity towards wind direction (no yawing mechanism required), illustrating them more cost-effective. The future scope includes utilizing the wind lens technology to increase the free-stream velocity entering the turbine, and hence, resulting in a higher power generation and efficiency.

6. References

[1] S.S. Dol, S. F. Wong, Y. K. Tiong, and M. A. Zahari, "The Feasibility of Wind and Solar Energy Application for Oil and Gas Offshore Platform," in 9th Curtin University of Technology Science and Engineering International Conference 2014 (CUTSE2014), Sarawak, 2014.

[2] T.J. Carrigan, B.H. Dennis, Z.X. Han, and B.P. Wang, "Aerodynamic Shape Optimization of a Vertical-Axis Wind Turbine using Differential Evolution," ISRN Renewable Energy, Vol. 2012, p. 16, 16 January 2012.

[3] N. Mishra, A. Jain, B. Khanna, and S. Mitra, "Experimental Investigation on a Ducted Savonius Vertical Axis Wind Turbine and its Performance Comparison with and without End-plates," Renewable Energy Research and Applications, Vol. 1, No. 1, 2020.

[4] A.A. Al Qubaisi, S.S. Dol, M.S. Khan, and A.A. Azeez, "Feasibility study and design of floating offshore wind turbine farm in United Arab Emirates," in 2018 Advances in Science and Engineering Technology International Conferences (ASET), 2018.

[5] I. Ibrahim, "Livable Eco-Architecture Masdar City, Arabian Sustainable City," Procedia - Social and Behavioral Sciences, Vol. 216, pp. 46 - 55, 21 January 2016.

[6] H.A. Riyami, A.A. Busaidi, A.A. Nadabi, M.A. Siyabi, O.H. Abdalla, K.A. Manthari, B. Hagenkort, S. Mirza, and R. Fahmi, "Power Quality of Dhofar Network with 50 MW Wind Farm Connection," in 2016 Eighteenth International Middle East Power Systems Conference (MEPCON), 2016.

[7] S.S. Dol, A.A. Azeez, A.A. Hasan, M. Alavi, and S.M. Khan, "Potential of Offshore Renewable Energy Applications in the United Arab Emirates," in Clean Energy Opportunities in Tropical Countries, Springer, 2021, pp. 237 - 265.

[8] F. Cugurullo and D. Ponzini, "The transnational smart city as urban eco-modernisation: the case of Masdar City in Abu Dhabi," in Inside Smart Cities: Place, Politics and Urban Innovation, Routledge, 2018, p. 14.

[9] A.A. Azeez, M. Gadala, N. Khudhiri, and S.S. Dol, "Aerodynamics Optimization of RC Plane Winglet," in 2019 8th International Conference on Modeling Simulation and Applied Optimization (ICMSAO), 2019.

[10] H. Riegler, "HAWT versus VAWT: Small VAWTs find a clear niche," Refocus, Vol. 4, No. 4, pp. 44-46, 22 August 2003.

[11] S. Mitchell, I. Ogbonna, and K. Volkov, "Improvement of Self-Starting Capabilities of Vertical Axis Wind Turbines with New Design of Turbine Blades," Sustainability, Vol. 13, No. 7, 31 March 2021.

[12] S.S. Dol and O.M. Kassem, "Feasibility Study of Offshore Wind and Solar Energy Technologies in the United Arab Emirates," International Journal of Engineering Research in Mechanical and Civil Engineering (IJERMCE), Vol. 5, No. 1, pp. 1 - 5, January 2020.

[13] P.I, Wind Turbine Design with Emphasis on Darrieus Concept, Vol. 1, Polytechnic International Press, 2002.

[14] L. Shuqin, "Magnetic Suspension and Self-pitch for Vertical-axis Wind Turbines," Fundamental and Advanced Topics in Wind Power, 5 July 2011.

[15] S. Sina, "Aero-Elastic Stability of Horizontal Axis Wind Turbine Blades," Renewable Energy Research and Applications, Vol. 2, No. 1, 23 June 2021.

[16] NREL, "File: Map United Arab Emirates speed," 12 Jan 2015.

[17] T.-t. Zhang, M. Elsakka, W. Huang, Z.-g. Wang, D. B. Ingham, L. Ma, and M. Pourkashanian, "Winglet design for vertical axis wind turbines based on a design of experiment and CFD approach," Energy Conversion and Management, Vol. 195, pp. 712 - 726, 1 September 2019.

[18] M. Javadi, A. Arab, M. Anbarsooz, and M. Moghiman, "A numerical study on the aerodynamic performance and the self-starting characteristics of a Darrieus wind turbine considering its moment of inertia," Renewable Energy, Vol. 107, pp. 298 - 311, 7 February 2017.

[19] S. Lain, M.A. Taborda and O.D. Lopez, "Numerical Study of the Effect of Winglets on the Performance of a Straight Blade Darrieus Water Turbine," Energies, Vol. 11, No. 2, p. 297, 28 January 2018.

[20] F. Arpino, G. Cortellessa, M. Dell'Isola, M. Scungio, V. Focanti, M. Profili, and M. Rotondi, "CFD simulations of power coefficients for an innovative Darrieus style vertical axis wind turbine with auxiliary

straight blades," in 35th UIT Heat Transfer Conference (UIT2017), Ancona, 2017.

[21] R. Dominy, P. Lunt, A. Bickerdyke, and J. Dominy, "Self-starting capability of a Darrieus turbine," Journal of Power and Energy, Vol. 221, No. 1, pp. 111 - 120, 14 September 2006.

[22] F.A. ElGhazali and S.S. Dol, "Aerodynamic Optimization of Unmanned Aerial Vehicle through Propeller Improvements," Journal of Applied Fluid Mechanics (JAFM), Vol. 13, No. 3, pp. 793 - 803, 29 September 2019.

[23] A.Q. Abdullah and S.S. Dol, "Aerodynamic Investigation and Design of Dimpled Surface Airfoil for UAV Propellers," in 2020 Advances in Science and Engineering Technology International Conferences (ASET), 2020.

[24] B. Eker, A. Akdogan, and A. Vardar, "Using of Composite Material in Wind Turbine Blades," Journal of Applied Sciences, Vol. 6, No. 14, pp. 2917 - 2921, 2006.

[25] W. A. Timmer and R. P. J. O. M. v. Rooij, "Summary of the Delft University Wind Turbine Dedicated Airfoils," Journal of Solar Energy Engineering, Vol. 125, No. 4, pp. 488 - 496, 26 November 2003.

[26] M. Islam, A. Fartaj, and R. Carriveau, "Analysis of the Design Parameters related to a Fixed-pitch Straight-Bladed Vertical Axis Wind Turbine," Sage Journals - Wind Engineering, Vol. 32, No. 5, p. 491 – 507, 1 October 2008.

[27] X. Cai, Y. Zhang, W. Ding, and S. Bian, "The aerodynamic performance of H-type darrieus VAWT rotor with and without winglets: CFD simulations," Energy Sources, Part A: Recovery, Utilization, and Environmental Effects, 20 June 2019.

[28] H.B. Chan, T.H. Yong, P. Kumar, S.K. Wee, and S.S. Dol, "The Numerical Investigation on the Effects of Aspect Ratio and Cross-sectional Shape on the Wake Structure behind a Cantilever," ARPN Journal of Engineering and Applied Sciences, Vol. 11, No. 16, August 2016.

[29] S.M.H. Karimian and A. Abdolahifar, "Performance investigation of a new Darrieus Vertical Axis Wind Turbine," Energy, Vol. 191, 15 January 2020.

[30] M. Islam, D. S.-K. Ting, and A. Fartaj, "Aerodynamic models for Darrieus-type straight-bladed vertical axis wind turbines," Renewable and Sustainable Energy Reviews, Vol. 12, No. 4, pp. 1087-1109, 28 December 2006.

[31] A. Untaroui, H.G. Wood, P.E. Allaire, and R.J. Ribando, "Investigation of Self-Starting Capability of Vertical Axis Wind Turbines using a Computational Fluid Dynamics Approach," Journal of Solar Energy Engineering, Vol. 133, No. 4, p. 8, 13 October 2011.

[32] A. Hasan, M.A. Iqbal, A.A. Azeez, N.M. Khudhiri, S.S. Dol, and M.S. Gadala, "Aerodynamics Analysis on Wings with Winglets and Vortex Generators," WSEAS Transactions on Fluid Mechanics, Vol. 15, December 2020.